WARSAW UNIVERSITY OF TECHNOLOGY Index 351733
FACULTY OF CIVIL ENGINEERING
COMMITTEE FOR CIVIL AND WATER ENGINEERING
POLISH ACADEMY OF SCIENCES ISSN 1230-2945
DOI: 10.24425/ace.2025.155116
ARCHIVES OF CIVIL ENGINEERING
Vol. LXXI ISSUE 3 2025
pp. 523–537

Research paper

Numerical investigation of steel-timber composite beams with cold-formed omega girders, part 1: non-modified beams

Marcin Chybiński[1], Anna Derlatka[2], Piotr Szewczyk[3], Piotr Lacki[4], Małgorzata Abramowicz[5], Łukasz Polus[6]

Abstract: This paper presents a preliminary evaluation of the load-bearing capacity of steel-timber composite beams with cold-formed omega girders and laminated veneer lumber slabs. These structural elements may be used as ceiling beams. The finite element models of the analysed composite beams were created in ADINA and Abaqus. The theoretical estimations of the resistance to bending were based on the elastic analysis (elastic resistance to bending) and the rigid-plastic theory (plastic resistance to bending). The elastic load-bearing capacity obtained in the numerical simulation in ADINA was identical to the one from the theoretical analysis. The elastic load-bearing capacity from the numerical analysis in Abaqus was 1.02 times higher than the one from the theoretical analysis. The plastic bending resistance obtained from the theoretical analysis was 1.08 times higher than the one from the numerical simulation in ADINA and 1.03 times higher than the one from the numerical simulation in Abaqus. In part 2 of the paper, a modification to the cross-section and a reinforcing method were proposed.

Keywords: laminated veneer lumber (LVL), omega cross-sections, steel-timber composite beams

[1]PhD., Eng., Poznan University of Technology, Faculty of Civil and Transport Engineering, Institute of Building Engineering, Piotrowo 5 Street, 60-965 Poznan, Poland, e-mail: marcin.chybinski@put.poznan.pl, ORCID: 0000-0003-2539-7764

[2]DSc., PhD., Eng., Czestochowa University of Technology, Department of Civil Engineering, Dabrowskiego 69 Street, Czestochowa, Poland, e-mail: anna.derlatka@pcz.pl, ORCID: 0000-0002-6509-2706

[3]PhD., Eng., West Pomeranian University of Technology in Szczecin, Faculty of Civil and Environmental Engineering, Al. Piastów 17, 70-310 Szczecin, Poland, e-mail: piotr.szewczyk@zut.edu.pl, ORCID: 0000-0002-2707-5630

[4]Prof., DSc., PhD., Eng., Czestochowa University of Technology, Department of Civil Engineering, Dabrowskiego 69 Street, Czestochowa, Poland, e-mail: piotr.lacki@pcz.pl, ORCID: 0000-0002-0787-8890

[5]PhD., Eng., West Pomeranian University of Technology in Szczecin, Faculty of Civil and Environmental Engineering, Al. Piastów 17, 70-310 Szczecin, Poland, e-mail: malgorzata.abramowicz@zut.edu.pl, ORCID: 0000-0002-4533-6953

[6]PhD., Eng., Poznan University of Technology, Faculty of Civil and Transport Engineering, Institute of Building Engineering, Piotrowo 5 Street, 60-965 Poznan, Poland, e-mail: lukasz.polus@put.poznan.pl, ORCID: 0000-0002-1005-9239

1. Introduction

Steel and timber have been used as building materials for years. However, the idea of combining steel and timber elements into a composite beam is relatively new and is related to the trend of sustainable construction. Steel-timber composite beams have several important benefits. The use of timber slabs instead of concrete slabs in floors can reduce the self-weight of structures, the construction time [1] and the embodied energy [2], while also improving the insulation performance of such structures [3]. The use of steel girders rather than timber girders in floors can increase the load-bearing capacity and decrease deflection. Demountable connectors can be used in steel-timber composite beams, allowing them to be deconstructed at the end of their service life [4]. Owing to the above advantages, steel-timber composite beams may be considered a sustainable solution for civil engineering [2, 5, 6]. Steel-timber composite structures were used for the construction of the bridge described in [7] and the dormitory presented in [8]. However, steel-timber composite structural elements also have some disadvantages. The standards for designing these structures have not yet been developed. However, a multi-disciplinary review of steel-timber structures was presented in Design Guide 37 [9]. The lighter weight of steel-timber composite elements comparted to steel-concrete composite elements is an advantage. However, it is also a serviceability drawback, which may result in poor performance of steel-timber composite floors [10–12]. The fire resistance of steel-timber composite beams should be analysed. To increase it, steel girders may be protected using fire-resistant materials.

Steel-timber composite beams have been the object of many investigations. In the solutions presented in the literature, timber slabs were made of engineered wood products, such as cross-laminated timber [13], laminated veneer lumber [14], glued-laminated timber [15], or particle board [16]. They were combined with hot-rolled [17], cold-formed [18] or welded [19] steel beams.

Kyvelou et al. [16, 18, 20] conducted experimental, theoretical and numerical analyses of steel-timber composite beams. The authors developed an analytical method for predicting the moment capacity of steel-timber composite beams with cold-formed steel girders. The method was based on the EN 1994-1-1 standard and took into account the attained degree of partial shear connection. The results based on this method were compared with the experimental and numerical results. It was found that the method yielded accurate predictions of the moment capacity. Hassanieh et al. conducted experimental and numerical investigations of steel-timber composite beams with LVL slabs and hot-rolled girders [21]. 1D and 2D numerical models of the beams were developed. The models captured the load-bearing capacity, failure mode, load-slip and load-deflection relations fairly well. The composite action was modelled using discrete shear connections. Chybiński and Polus investigated aluminium-timber composite beams with screwed connections [22]. A 3D numerical model with discrete shear connections was developed and the ratio of the load-bearing capacity from the numerical simulation to the mean value from the laboratory tests was 0.95. The plastic resistance to bending of the beam was calculated based on the rigid-plastic theory and the EN 1994-1-1 standard. The ratio of the load-bearing capacity from the theoretical model to the mean value from the tests was 1.07.

Recently, innovative steel-timber composite beams with omega-shaped and U-shaped cross-section girders have been developed (Fig. 1 [23–25]).

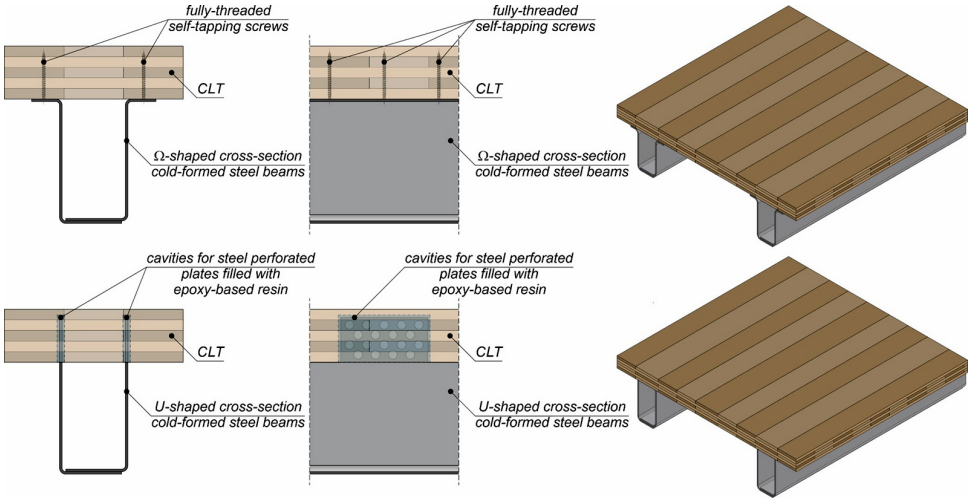

Fig. 1. Steel-timber composite beams with omega-shaped and U-shaped cross-section girders developed by Loss and Davison [23]

In the solution presented in [23], two steel girders were joined with a CLT panel to create a prefabricated steel-timber composite component. Such components may be used to develop innovative floors. They are easy to assemble and deconstruct. The experimental bending tests on the modular components yielded valuable results. However, only steel-timber composite components with CLT panels were tested. Furthermore, the omega-shaped cross-section girder was manufactured by welding together two cold-formed profiles. The girder was 4 mm thick and therefore it was not thin-walled.

In this paper, steel-timber composite beams with cold-formed omega girders and LVL slabs instead of CLT panels were studied. The omega-shaped cross-section girder was made as one cold-formed profile instead of two. The height, thickness and length of the omega girders analysed in this paper is different than in the paper presented by Loss and Davison [23]. The purpose of this research work was to evaluate the resistance to bending of non-modified composite beams. In part 2 of the paper, a modification to the cross-section as well as a reinforcing method were proposed.

2. Materials and methods

2.1. The LVL slab

In the LVL slab used in this study (45 mm × 300 mm × 3000 mm), all veneers were glued lengthwise. The mechanical properties of the LVL as declared by the manufacturer in [26] were taken into account in the theoretical estimations and numerical models. LVL is an

engineered timber composite consisting of wood veneers [27]. It is manufactured in a factory under controlled conditions and defects are eliminated or evenly distributed [28]. LVL may be manufactured from trees of small diameters using the rotary peeling method. Structural elements made of LVL may be strengthened using carbon fibre reinforced polymer strips [29]. Recently, Bakalarz and Kossakowski have demonstrated the effectiveness of combining LVL with fibre reinforced polymer sheets (FRP) and have indicated that the properties of FRP and LVL have an impact on the effectiveness of the reinforcement [30].

2.2. The steel girder

The omega girder was a 3-mm-thick cold-formed profile made of S235 grade steel. Its mechanical properties were based on the EN 1993-1-1 standard [31]. It was made as one cold-formed profile. Relatively thin structural elements allow for the more optimal use of steel [32, 33]. The interaction between cold-formed beams and other elements has been the object of many investigations [16, 34].

2.3. The steel-timber composite beam without a modification or reinforcement

The authors analysed a simply-supported steel-timber composite beam with a cold-formed omega girder and an LVL slab subjected to a four-point bending test. Figure 2 presents the geometric configurations of the reference composite beam.

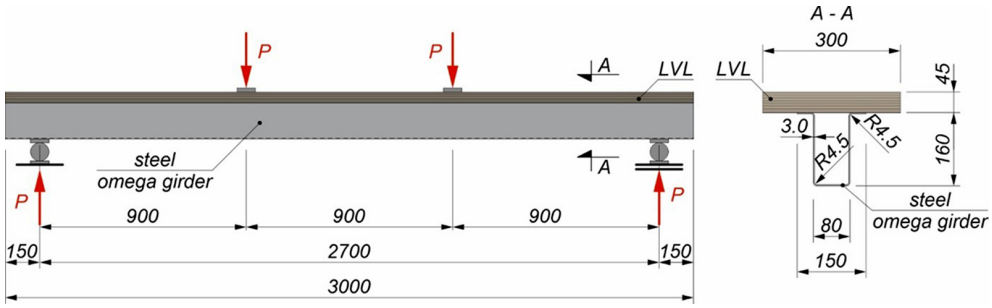

Fig. 2. The simply-supported steel-timber composite beam analysed in this paper

The authors are also planning to conduct laboratory tests of steel-timber composite beams with cold-formed omega girders. The dimensions of the future test stand were taken into account when determining the length of the beam and the width of the slab used in the present analysis.

3. A theoretical analysis of the non-modified beam

The elastic and plastic theoretical resistance to bending of the steel-timber composite beam were calculated based on the methods developed for steel-concrete composite elements presented in the EN 1994-1-1 standard [35] (Fig. 3).

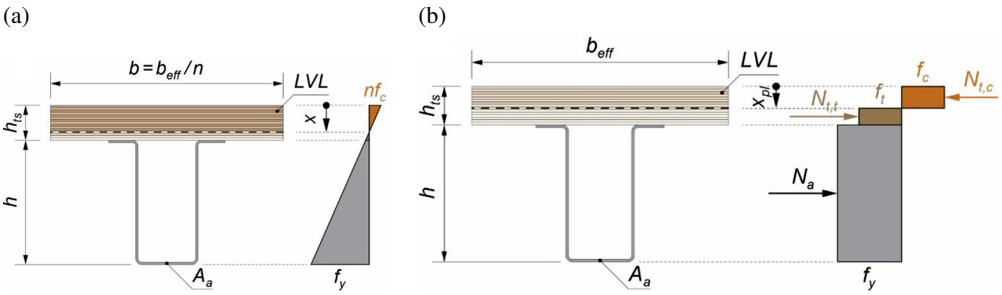

Fig. 3. The models used to calculate: (a) the elastic resistance to bending, (b) the plastic resistance to bending

These methods were also used in the analyses of aluminium-timber and steel-timber composite beams presented in the literature [22, 36, 37]. The elastic resistance to bending of the analysed beam was evaluated with the following assumptions: the normal stress in the cold-formed omega girder flange did not exceed the yield strength of the steel, and the normal stress in the LVL slab did not exceed the compressive strength of the LVL. The cross-section of the steel-timber composite beam was replaced with an ideal cross-section. The width of the slab in the ideal cross-section was reduced because the ratio of the modulus of elasticity of steel to the modulus of elasticity of LVL (n) was used (Table 1).

Table 1. The elastic resistance to bending of the steel-timber composite beam with a cold-formed omega girder and an LVL slab

Parameter	Value
n ratio	15.0
Width of the ideal LVL slab b, mm	20.0
Position of the neutral axis measured from the top edge of the LVL slab x, mm	85.2
Second moment of area of the ideal cross-section I, cm^4	1067.5
Elastic resistance to bending M_{el}, kN · m	20.9

The plastic resistance to bending of the analysed beam was calculated based on the rigid-plastic theory. The part of the LVL slab subjected to tension was taken into account in the calculations of the plastic resistance to bending (Table 2).

Table 2. The plastic resistance to bending of the steel-timber composite beam with a cold-formed omega girder and an LVL slab

Parameter	Value
Cross-section area of the omega girder A_a, cm^2	13.92
Steel yield strength f_y, MPa [31]	235.0
LVL compressive strength f_c, MPa [26]	40.0
LVL tension strength f_t, MPa [26]	36.0
Effective width of the LVL slab b_{eff}, mm	300.0
Height of the LVL slab h_{ts}, mm	45
Height of the omega girder h, mm	160
Position of the plastic axis measured from the top edge of the LVL slab x_{pl}, mm	35.7
Plastic resistance to bending M_{pl}, kN · m	37.2

The equations used for x_{pl} and M_{pl} calculations were presented in [22] and different scenarios (e.g., when the depth of the compressive zone is greater than the depth of the LVL slab) were discussed in [37].

4. Numerical models

The finite element method was used to develop numerical models of the composite beams. Simulations were carried out using the Abaqus and ADINA programs. In part 1 of the paper, numerical models of the reference beam were developed using both programs, and the results were compared. In part 2 of the paper, a numerical model of the beam reinforced with carbon fibre reinforced polymer (CFRP) tapes was created in Abaqus and a numerical model of the beam with steel sheets was developed in ADINA.

In each numerical model, the LVL slab was simulated using 3D solid finite elements, while the steel beam and the CFRP tape were modelled using shell finite elements. The central surface of the sheet metal from which the omega section was made was included in the models, the CFRP tape was modelled (in part 2 of the paper) in an identical way.

To take into account the thickness of the steel section (3.0 mm), the beam was moved 1.5 mm away from the slab. The shape of the steel beam used in the numerical models is presented in Fig. 4.

The support plates and the plates under the actuators were simulated using 3D solid finite elements in the ADINA program and shell elements in the Abaqus program. Bilinear elastic-plastic material models were used for the simulation of all components. Nominal property values of materials were used. The steel properties were based on the Eurocode 3 standard [31]. The compressive strength, i.e., 40 MPa, was used as the strength of the LVL [26]. The adopted values are presented in Fig. 5 and Table 3.

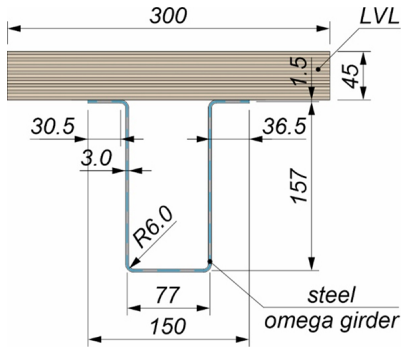

Fig. 4. The cross-section of the steel-timber composite beam used in the numerical simulations

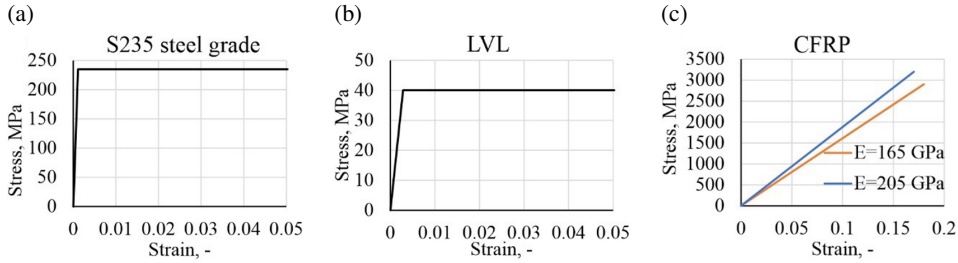

Fig. 5. The material model used in the numerical simulations: (a) steel, (b) LVL, (c) CFRP

Table 3. Material properties used in the numerical models

Property	**Steel [31]**	**LVL [22,26]**	**CFRP tape – type 1 [38]**	**CFRP tape – type 2 [39]**
Young's modulus E, GPa	210	14	165	205
Yield strength f_y, MPa	235	40	2900	3200
Poisson's ratio ν	0.3	0.48	0.3	0.3
Density ρ, kg/m^3	7850	550	1600	1600

Self-weight was taken into account in the numerical models, while the mesh size was 15 mm. The bilinear elastic-plastic material models were used to evaluate the load-bearing capacity of the composite beam in accordance with Eurocode 4 [35] and the rigid-plastic theory. The elastic-perfectly plastic material model did not need many input parameters. However, it did not take the LVL failure and its anisotropy into account. In paper [40], Chybiński and Polus used two models for LVL. In the first one, they modelled LVL as an elastic-perfectly plastic material. In the second one, they modelled LVL as an orthotropic material and captured its failure using the Hashin damage model. However, the second model required many input parameters. The load-carrying capacity of the LVL structural element from the finite element

analysis for the first material model (11.6 kN · m) was 8% higher than in the second model (10.7 kN · m) and 7% lower than in the laboratory tests (12.4 kN · m).

The connection between the LVL slab and the steel girder was rigid, and it was simulated on the entire contact surface between the finite elements reflecting the individual components of the composite beam. For this reason, the developed numerical model represented the composite beam with full shear connection. Future studies should take into account the impact of connection flexibility.

4.1. The model of the non-modified beam in the Abaqus program

The numerical model of the steel-timber composite beam consisted of a steel beam, an LVL slab, and load and support plates (Fig. 6).

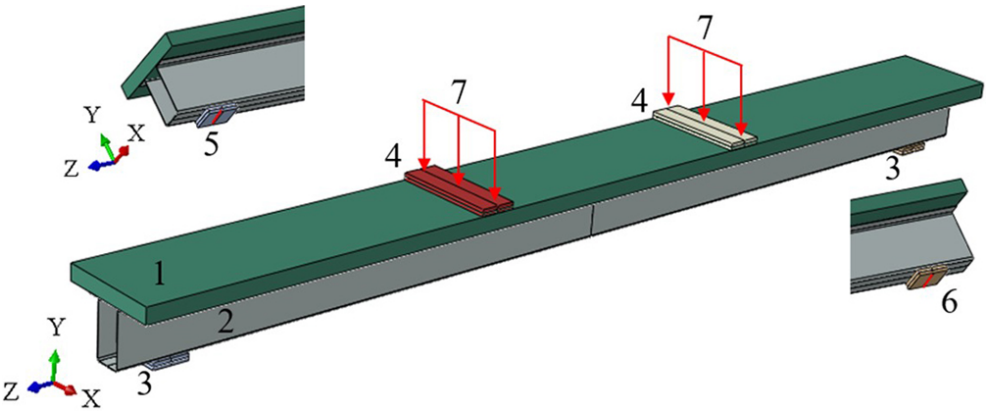

Fig. 6. The numerical model in the Abaqus program: 1 – LVL slab, 2 – steel beam, 3 – support plate, 4 – load plate, 5 – displacement in x, y and z directions (fixed), 6 – displacement in x and y directions (fixed), 7 – displacement in y direction

The LVL slab was divided into twenty-node cuboidal finite solid elements (C3D20), while the steel beam and the plates were divided into eight-node shell elements (S8R). The LVL slab and the steel beam were connected using a tie function. For this reason, the developed numerical model represented the composite beam with a full shear connection. The interaction between the composite beam parts and the steel plates was captured using surface-to-surface "hard" and friction contacts. In the case of the steel–steel interface, a friction coefficient equal to 0.45 was used, and in the case of the LVL–steel interface, the friction coefficient was equal to 0.3 [21].

4.2. The model of the non-modified beam in the ADINA program

In the numerical model of the composite beam (Fig. 7), a non-linear analysis taking into account large displacements and strains was conducted.

The LVL slabs as well as the support plates and the plates under the actuators were discretized by 20-node 3D solid elements. The steel omega beam was discretized by 8-node

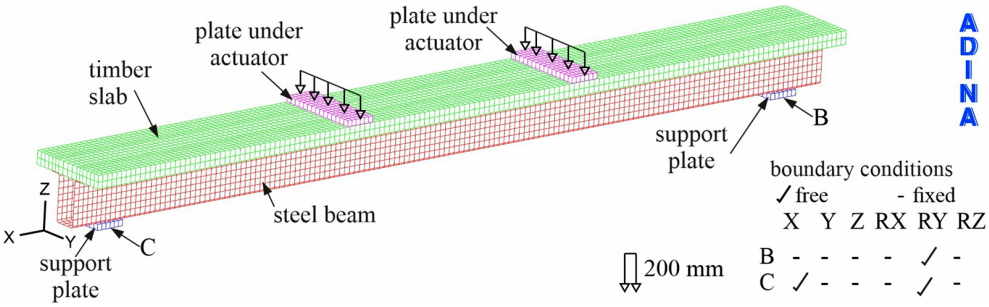

Fig. 7. The numerical model in ADINA

shell elements. The components of the simulated steel-timber composite beam were connected using the "glue mesh" contact method. The mesh glueing procedure involves joining two surfaces with different finite element meshes. Glueing ensures adhesion between the glued surfaces and a smooth transition of displacements. The interactions between the components in the finite element models were as follows:

– the upper surface of the steel beam and the lower surface of the LVL slab,
– the upper surface of the LVL slab and the lower surfaces of the plates under the actuators,
– the lower surface of the steel beam and the upper surfaces of the support plates.

The sensitivity analysis of the mesh size was performed using the numerical model developed in ADINA. The following five variants were analysed: 15, 20, 30, 40 and 50 mm. The authors analysed the deflection – bending moment curves (Fig. 8a) as well as the values of reaction and deflection (Fig. 8b) under the 200 mm displacement acting on each actuator.

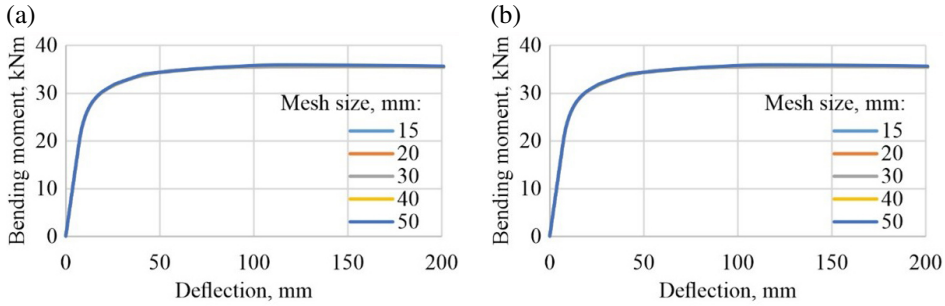

Fig. 8. The sensitivity analysis of the mesh size: (a) deflection–bending moment curves, (b) reaction and deflection reference values

The summary of the obtained and relative values is presented in Table 4.

The results from the model with the 15 mm mesh were used as reference points and therefore each relative value for this model was 100%. The deflection–bending moment curves (Fig. 8a) were almost identical – the differences between the curves were hardly noticeable. Some small differences can be observed in Table 4. The reactions and deflections of the

Table 4. The results of the sensitivity analysis

Parameter	Value					Relative value				
Mesh size, mm	15	20	30	40	50	15	20	30	40	50
Reaction, kN	39.60	39.59	39.59	39.91	39.92	100.0%	100.0%	100.0%	100.8%	100.8%
Deflection, mm	241.6	242.6	241.7	242.4	249.4	100.0%	100.4%	100.0%	100.3%	103.2%
Computational time, s	1953	827	361	185	162	100.0%	42.4%	18.5%	9.5%	8.3%

composite beam modelled using the elements with the mesh size of 15, 20, 30 and 40 mm are comparable (Fig. 8b). The differences in the values are less than one percentage point. The bigger differences in deflection (of a few percentage points) are observed in the model with the 50 mm mesh size. Therefore, to analyse a composite beam with a relatively small number of finite elements and interactions between them (the connections were modelled in a simplified manner), the model with the 15 mm mesh calculated over a longer time could be used. However, for a more complicated numerical model, the mesh size of 20 mm or 30 mm with a shorter computational time can also be applied.

5. Results

The elastic and plastic load-bearing capacity from the theoretical analysis and the bending moment – deflection curves from the FEM simulations in the ADINA and Abaqus programs are presented in Fig. 9.

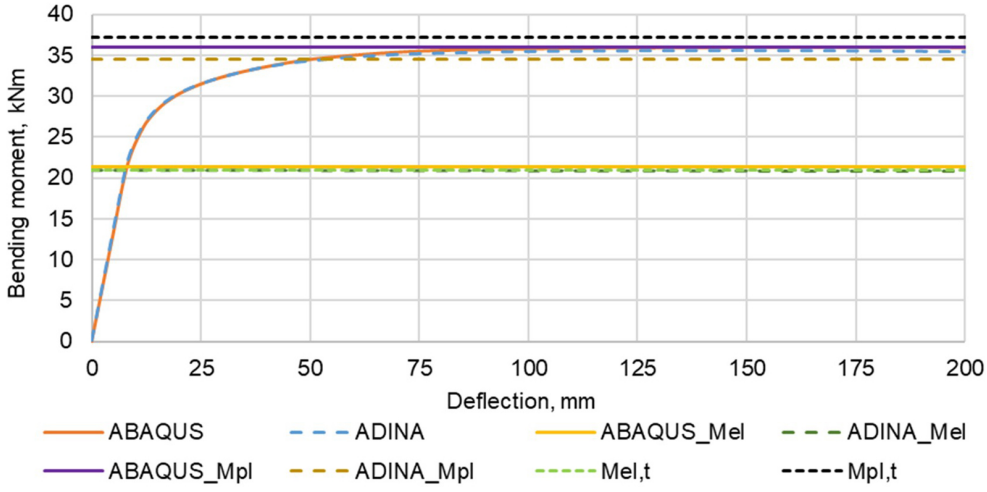

Fig. 9. The bending moment–deflection curves from the numerical analyses of the reference beam

It is evident that the curves obtained in both programs overlap. The elastic load-bearing capacity (Table 5) obtained in the numerical simulation in ADINA (Fig. 10a) is identical to the one from the theoretical analysis.

Table 5. A comparison of the elastic and plastic load-bearing capacity of the reference beam

Property	Theoretical	ADINA	Abaqus
Elastic load-bearing capacity M_{el}, kNm	20.9	20.9	21.3
Plastic load-bearing capacity M_{pl}, kNm	37.2	34.5	36.0

The elastic load-bearing capacity from the numerical analysis in Abaqus (Fig. 10b) is 1.02 times higher than the one from the theoretical analysis.

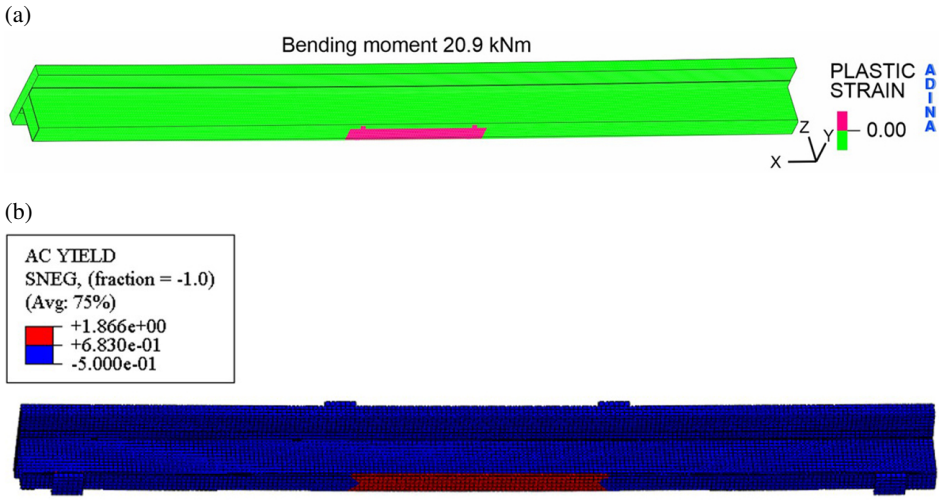

Fig. 10. The yield strength achieved at the bottom flange of the omega girder: (a) in the ADINA program (M = 20.9 kN · m); (b) in the Abaqus program (M = 21.3 kN · m)

Greater differences are visible when the values of the plastic load-bearing capacity (Table 5) are compared. The values of the plastic load-bearing capacity obtained from the numerical simulations (34.5 kN · m and 36.0 kN · m) presented in Fig. 11 are lower than the result from the theoretical analysis (37.2 kN · m).

The differences are below 8%. The peaks and the descending parts of the curves are not clearly visible in Fig. 9 because the LVL model did not take into account the LVL damage. Future numerical analyses should take into account the impact of the LVL damage.

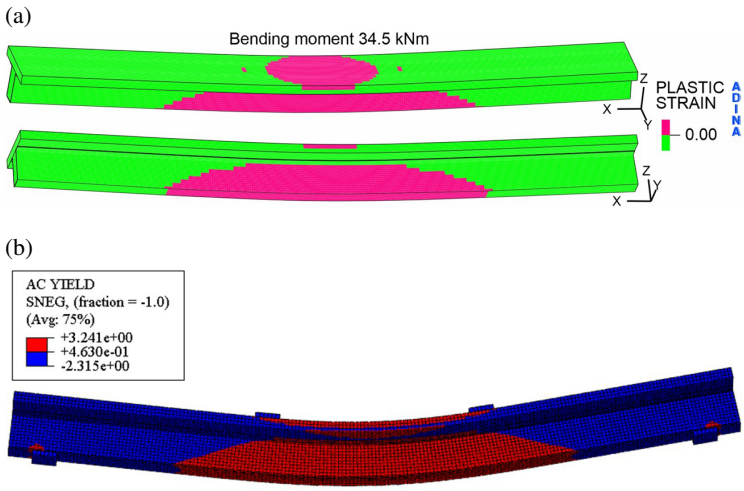

Fig. 11. The yield strength achieved in the omega girder and the resistance of the LVL achieved on the top and bottom edges of the slab: (a) in the ADINA program (M = 34.5 kN · m); (b) in the Abaqus program (M = 36.0 kN · m)

6. Conclusions

In this paper, non-modified steel-timber composite beams with cold-formed omega girders were investigated. The elastic load-bearing capacity obtained from the theoretical analysis was identical to the one from the numerical simulation in ADINA and 1.02 times lower than the one from the numerical simulation in Abaqus. The plastic bending resistance obtained from the theoretical analysis was 1.08 times higher than the one from the numerical simulation in ADINA and 1.03 times higher than the one from the numerical simulation in Abaqus.

The investigation presented in this paper has certain limitations. Only theoretical and numerical analyses of the beams with full composite action were conducted. The impact of slipping on the stiffness and load-bearing capacity of the steel-timber composite beams with cold-formed omega girders was not taken into account. Furthermore, the simple model (elastic-perfectly plastic material model) was used to capture the behaviour of LVL. Future numerical analyses should take into account the impact of the LVL damage and its anisotropy. Due to the above limitations, the presented investigation was only a preliminary evaluation of the load-bearing capacity of the steel-timber composite beams. The authors of this paper plan to conduct laboratory tests of steel-timber composite beams with cold-formed omega girders. The results of the laboratory tests will be used to create and validate advanced numerical models.

References

[1] A. Romero and C. Odenbreit, "Experimental investigation on novel shear connections for demountable steel-timber composite (STC) beams and flooring systems", *Engineering Structures*, vol. 304, art. no. 117620, 2024, doi: 10.1016/j.engstruct.2024.117620.

[2] A.A. Chiniforush, A. Akbarnezhad, H. Valipour, and J. Xiao, "Energy implications of using steel-timber composite (STC) elements in buildings", *Energy and Buildings*, vol. 176, pp. 203–215, 2018, doi: 10.1016/j.enbuild.2018.07.038.

[3] X. Song, L. Zhao, Y. Liu, and M. Gong, "Experimental and nonlinear analytical of the flexural performance of timber-filled steel tubular composite beams", *Engineering Structures*, vol. 301, art. no. 117312, 2024, doi: 10.1016/j.engstruct.2023.117312.

[4] A. Ataei, A.A. Chiniforush, M. Bradford, and H. Valipour, "Cyclic behaviour of bolt and screw shear connectors in steel-timber composite (STC) beams", *Journal of Constructional Steel Research*, vol. 161, pp. 328–340, 2019, doi: 10.1016/j.jcsr.2019.05.048.

[5] M. Abramowicz, M. Chybiński, Ł. Polus, P. Szewczyk, and T. Wróblewski, "Dynamic Response of Steel–Timber Composite Beams with Varying Screw Spacing", *Sustainability*, vol. 16, no. 9, art. no. 3654, 2024, doi: 10.3390/su16093654.

[6] M.A. Bradford, A. Hassanieh, H.R. Valipour, and S.J. Foster, "Sustainable Steel-timber Joints for Framed Structures", *Procedia Engineering*, vol. 172, pp. 2–12, 2017, doi: 10.1016/j.proeng.2017.02.011.

[7] B. Bakht and R. Krisciunas, "Testing a Prototype Steel-Wood Composite Bridge", *Structural Engineering International*, vol. 7, no. 1, pp. 35–41, 1997, doi: 10.2749/101686697780495391.

[8] D.J. Odeh and P. Kuehnel, "The Hybrid CLT Steel Residence Hall", *Structure*, 2019. [Online]. Available: https://www.structuremag.org/article/the-hybrid-clt-steel-residence-hall/.

[9] D. Barber, D. Blount, J.J. Hand, M. Roelofs, L. Wingo, J. Woodson, and F. Yang, *Design Guide 37: Hybrid Steel Frames with Wood Floors*. American Institute of Steel Construction, 2022.

[10] P. Hamm, A. Richter, and S. Winter, "Floor vibrations–new results", in *11th World Conference on Timber Engineering (WCTE 2010)*, A. Ceccotti, Ed. Trentino, 2010.

[11] B. Chocholaty, N.B. Roozen, M. Maeder, and S. Marburg, "Vibroacoustic response of steel–timber composite elements", *Engineering Structures*, vol. 271, art. no. 114911, 2022, doi: 10.1016/j.engstruct.2022.114911.

[12] A. Chiniforush, M. Makki Alamdari, U. Dackermann, H.R. Valipour, and A. Akbarnezhad, "Vibration behaviour of steel-timber composite floors, part (1): Experimental & numerical investigation", *Journal of Constructional Steel Research*, vol. 161, pp. 244–257, 2019, doi: 10.1016/j.jcsr.2019.07.007.

[13] A. Hassanieh, H.R. Valipour, and M.A. Bradford, "Load-slip behaviour of steel-cross laminated timber (CLT) composite connections", *Journal of Constructional Steel Research*, vol. 122, pp. 110–121, 2016, doi: 10.1016/j.jcsr.2016.03.008.

[14] A. Romero, J. Yang, F. Hanus, and C. Odenbreit, "Numerical Investigation of Steel-LVL Timber Composite Beams", *ce papers*, vol. 5, no. 2, pp. 21–30, 2022, doi: 10.1002/cepa.1694.

[15] Y. Zhao, Y. Yuan, C.-L. Wang, and S. Meng, "Experimental and finite element analysis of flexural performance of steel-timber composite beams connected by hybrid-anchored screws", *Engineering Structures*, vol. 292, art. no. 116503, 2023, doi: 10.1016/j.engstruct.2023.116503.

[16] P. Kyvelou, L. Gardner, and D.A. Nethercot, "Design of Composite Cold-Formed Steel Flooring Systems", *Structures*, vol. 12, pp. 242–252, 2017, doi: 10.1016/j.istruc.2017.09.006.

[17] A. Hassanieh, H.R. Valipour, and M.A. Bradford, "Experimental and analytical behaviour of steel-timber composite connections", *Construction and Building Materials*, vol. 118, pp. 63–75, 2016, doi: 10.1016/j.conbuildmat.2016.05.052.

[18] P. Kyvelou, L. Gardner, and D.A. Nethercot, "Testing and Analysis of Composite Cold-Formed Steel and Wood-Based Flooring Systems", *Journal of Structural Engineering*, vol. 143, no. 11, 2017, doi: 10.1061/(ASCE)ST.1943-541X.0001885.

[19] R. Liu, J. Liu, Z. Wu, L. Chen, and J. Wang, "A Study on the Influence of Bolt Arrangement Parameters on the Bending Behavior of Timber–Steel Composite (TSC) Beams", *Buildings*, vol. 12, no. 11, art. no. 2013, 2022, doi: 10.3390/buildings12112013.

[20] P. Kyvelou, L. Gardner, and D.A. Nethercot, "Finite element modelling of composite cold-formed steel flooring systems", *Engineering Structures*, vol. 158, pp. 28–42, 2018, doi: 10.1016/j.engstruct.2017.12.024.

[21] A. Hassanieh, H.R. Valipour, and M.A. Bradford, "Experimental and numerical study of steel-timber composite (STC) beams", *Journal of Constructional Steel Research*, vol. 122, pp. 367–378, 2016, doi: 10.1016/j.jcsr.2016.04.005.

[22] M. Chybiński and Ł. Polus, "Theoretical, experimental and numerical study of aluminium-timber composite beams with screwed connections", *Construction and Building Materials*, vol. 226, pp. 317–330, 2019, doi: 10.1016/j.conbuildmat.2019.07.101.

[23] C. Loss and B. Davison, "Innovative composite steel-timber floors with prefabricated modular components", *Engineering Structures*, vol. 132, pp. 695–713, 2017, doi: 10.1016/j.engstruct.2016.11.062.

[24] C. Loss and A. Frangi, "Experimental investigation on in-plane stiffness and strength of innovative steel-timber hybrid floor diaphragms", *Engineering Structures*, vol. 138, pp. 229–244, 2017, doi: 10.1016/j.engstruct.2017.02.032.

[25] D. Owolabi and C. Loss, "Experimental and numerical study on the bending response of a prefabricated composite CLT-steel floor module", *Engineering Structures*, vol. 260, art. no. 114278, 2022, doi: 10.1016/j.engstruct.2022.114278.

[26] M. Komorowski, *Podręcznik Projektowania i Budowania w Systemie STEICO. Podstawy. Fizyka Budowli. Zalecenia Wykonawcze*. Warsaw: Forestor Communication, 2020.

[27] J. Porteous and A. Kermani, *Structural Timber Design to Eurocode 5*, 2nd ed. Chichester: Wiley-Blackwell, 2013.

[28] M.W. Hammad, H.R. Valipour, T. Ghanbari-Ghazijahani, and M.A. Bradford, "Timber-timber composite (TTC) beams subjected to hogging moment", *Construction and Building Materials*, vol. 321, art. no. 126295, 2022, doi: 10.1016/j.conbuildmat.2021.126295.

[29] M. Bakalarz, "Load bearing capacity of laminated veneer lumber beams strengthened with CFRP strips", *Archives of Civil Engineering*, vol. 67, no. 3, pp. 139–155, 2021, doi: 10.24425/ace.2021.138048.

[30] M.M. Bakalarz and P.G. Kossakowski, "Strengthening of Laminated Veneer Lumber Slabs with Fiber-Reinforced Polymer Sheets – Preliminary Study", *Fibers*, vol. 12, no. 3, 2024, doi: 10.3390/fib12030022.

[31] Eurocode 3: Design of steel structures - Part 1–1: General rules and rules for buildings. European Committee For Standardization, 2006.

[32] N. Staszak, T. Gajewski, and T. Garbowski, "Effective Stiffness of Thin-Walled Beams with Local Imperfections", *Materials*, vol. 15, no. 21, art. no. 7665, 2022, doi: 10.3390/ma15217665.

[33] T. Gajewski, N. Staszak, and T. Garbowski, "Parametric Optimization of Thin-Walled 3D Beams with Perforation Based on Homogenization and Soft Computing", *Materials*, vol. 15, no. 7, art. no. 2520, 2022, doi: 10.3390/ma15072520.

[34] K. Ciesielczyk and R. Studziński, "Experimental investigation of sandwich panels supported by thin-walled beams under various load arrangements and number of connectors", *Archives of Civil Engineering*, vol. 68, no. 4, pp. 389–402, 2022, doi: 10.24425/ace.2022.143045.

[35] Eurocode 4: Design of composite steel and concrete structures - Part 1–1: General rules and rules for buildings. European Committee For Standardization, 2008.

[36] M. Chybiński and Ł. Polus, "Experimental and numerical investigations of aluminium-timber composite beams with bolted connections", *Structures*, vol. 34, pp. 1942–1960, 2021, doi: 10.1016/j.istruc.2021.08.111.

[37] J. Strzelecka, Ł. Polus, and M. Chybiński, "Theoretical and Numerical Analyses of Steel-timber Composite Beams with LVL Slabs", *Civil and Environmental Engineering Reports*, vol. 33, no. 2, pp. 64–84, 2023, doi: 10.59440/ceer/172510.

[38] Product Information: Card Sika®CarboDur®S. [Online]. Available: www.sika.com/dam/dms/plcon/s/sika_carbodur_s.pdf.

[39] Product Information: Card Sika®CarboDur®M. [Online]. Available: www.sika.com/dam/dms/plcon/5/sika_carbodur_m.pdf.

[40] M. Chybiński and Ł. Polus, "Experimental and numerical investigations of laminated veneer lumber panels", *Archives of Civil Engineering*, vol. 67, no. 3, pp. 351–372, 2021, doi: 10.24425/ace.2021.138060.

Badania numeryczne belek zespolonych stalowo-drewnianych z dźwigarami zimnogiętymi o przekroju w kształcie litery omega, część 1: belki bez modyfikacji

Słowa kluczowe: belki zespolone stalowo-drewniane, drewno klejone warstwowo z fornirów (LVL), przekroje w kształcie litery omega

Streszczenie:

Artykuł przedstawia wstępną analizę nośności belek zespolonych stalowo-drewnianych z dźwigarami zimnogiętymi o przekroju w kształcie litery omega oraz z płytami z drewna klejonego warstwowo z fornirów. Elementy te mogą być wykorzystywane jako belki stropowe. Modele numeryczne analizowanych belek zespolonych zostały wykonane w programach ADINA oraz Abaqus. Teoretyczna nośność na zginanie w zakresie sprężystym została wyznaczona na podstawie analizy sprężystej, a teoretyczna nośność na zginanie w zakresie plastycznym została obliczona na podstawie analizy sztywno-plastycznej. Nośność na zginanie w zakresie sprężystym wyznaczona na podstawie analizy numerycznej w programie ADINA była taka sama jak nośność teoretyczna, a nośność na zginanie w zakresie sprężystym wyznaczona w programie Abaqus była 1,02 razy większa niż nośność otrzymana na podstawie analizy teoretycznej. Nośność na zginanie w zakresie plastycznym otrzymana z analizy teoretycznej była 1,08 razy większa niż nośność otrzymana na podstawie symulacji w programie ADINA oraz 1,03 razy większa niż nośność z analizy numerycznej w programie Abaqus. W 2 części pracy zaproponowano modyfikację przekroju belki oraz sposób jej wzmacniania.

Received: 2024-08-08, Revised: 2024-10-28